



Contents lists available at ScienceDirect

Composites: Part B

journal homepage: www.elsevier.com/locate/compositesb

Effect of alumina, silk and ceria short fibers in reinforcement of Bis-GMA/TEGDMA dental resin



Arun Prabhu Rameshbabu, Saralashrita Mohanty^{1,2}, Kamakshi Bankoti¹, Paulomi Ghosh¹, Santanu Dhara^{*}

Biomaterials and Tissue Engineering Laboratory, School of Medical Science and Technology, Indian Institute of Technology Kharagpur, Kharagpur 721302, India

ARTICLE INFO

Article history:

Received 27 March 2014

Received in revised form 10 November 2014

Accepted 14 November 2014

Available online 22 November 2014

Keywords:

- A. Fibers
- A. Resins
- B. Cure behaviour
- B. Mechanical properties

ABSTRACT

The present study is focused to investigate influence of short fibers such as Alumina Microfibers (AMFs), Silk Microfibers (SMFs) and Ceria Nanofibers (CNFs) as reinforcements in Bis-GMA/TEGDMA resin towards development of composite dental filler. Morphologies of AMFs, SMFs, CNFs and their representative fracture surfaces of the reinforced dental resins/composites were examined by SEM. X-ray Diffraction Analysis was done to analyse the phase of the fibers used in this study and degree-of-conversion of the fiber incorporated base resin was studied by FTIR. Viscosity study of fiber resin mixture, depth of cure and mass change behaviour of the fibers resin composites in artificial saliva were done to analyse the flow ability and physical properties of the fiber resin composites. Mechanical properties of the composites were tested by a universal testing machine. This study demonstrated that incorporation of 10% AMFs, 5% SMFs, and 3.33% CNFs individually in Bis-GMA/TEGDMA dental resin resulted in similar degree of conversion compared to the control. Also the fiber reinforced composites (10% AMFs, 5% SMFs, and 3.33% CNFs) demonstrated significant improvement in mechanical properties compared to Bis-GMA/TEGDMA resin (Control). However, depth of cure was significantly reduced due to incorporation of fibers in the resin. The reinforcement effect of AMFs, SMFs in dental resin was superior due to their uniform distribution and good interfacial bonding between fibers and resin matrix. In case of CNFs, rapid increase in viscosity during mixing of fibers with resin and inhomogeneous mixing were the major problem encountered during formulation, which was mainly associated with high surface to volume ration of the nanofibers. The resultant composite containing CNFs had less improvement in mechanical properties which may be due to less fiber content, formation of agglomerates and improper distribution of the fibers in the composite which subsequently resulted in reduction of adhesive strength.

© 2014 Elsevier Ltd. All rights reserved.

1. Introduction

Restoration dentistry during progression of dental carries is important to prevent early tooth loss [1]. In this context, different dental filler materials were explored to identify a reliable composition with required physical and mechanical properties. Amalgam alloys were widely used as dental filler for several decades [2]. However, they suffer from certain drawbacks such as toxicity, environmental pollution, inadequate bioactivity and lack of aesthetic appearance [3–5]. Compared to the dental amalgams, the Resin Based Composites (RBC) are reported to possess better aesthetic property, less safety concern, and clinically effective [6–8]. Although

2,2-bis[4-(20-hydroxy-30-ethacryloyloxypropoxy)phenyl]propane (Bis-GMA) is the base monomer most commonly used in restorative materials, it is very high viscosity ($>10^3$ Pa s) results in limited loadings of reinforcement fillers and low final conversions of homopolymerized Bis-GMA. Therefore, a reactive diluent, such as triethylene glycol dimethacrylate (TEGDMA), is often added to reduce the viscosity and improve both the reactivity and the final conversion by adding vinyl monomer [9].

Dental composites serve under wet oral environment and should have the ability to withstand various stresses during chewing. Also, the compressive strength of the composite has to be high enough so that the filling does not fail, when the restoration is subjected to bending load. Further, it should withstand high compressive forces in the teeth, which can go up to 800 N. They should have flexural strength in the range of 100–140 MPa, which can fulfil the benchmark of small restorations [10]. The relatively high polymerization shrinkage, lack of adhesion to dentine, brittleness, poor marginal adaptation, inadequate fracture resistance and lack of

^{*} Corresponding author. Tel.: +91 3222 282306.

E-mail address: sdhara@smst.iitkgp.ernet.in (S. Dhara).

¹ Authors contributed equally.

² Present address: School of Mechanical & Building Sciences, Vellore Institute of Technology University, Vellore 632014, India.

caries-protective properties of light cured resin based composites hinder their use in large stress-bearing restorations such as direct posterior restorations involving cusps, and indirect crown and multiple-unit restorations [11]. Another problem associated with the use of light cured resin composite directly in the posterior region is the decrease in curing-light intensity with depth in the material. It is thus important to achieve sufficient irradiance on the bottom surface of each of the incremental layers used in building up the restoration [12]. Inadequate polymerization along the depth of the restoration can lead to undesirable effects, e.g. gap formation, marginal leakage, recurrent caries, adverse pulpal effects and ultimate failure of the filler [13]. Also, the strength of dental composites decreases significantly after long-term water aging. The average lifetime of dental composites is less than 5 years. In this context, dental resin composites need to be strengthened in order to improve their performance.

Reason proposed for the failure of composites is due to the poor adhesion between the fillers and the matrix. Good bonding between fillers and the resin matrix is vital in composites to improve their mechanical and physical properties. Filler size is one of the critical factors affecting the overall properties of a resin-composite. The filler shape, amount, constituents of filler particles employed in dental composites have been identified to influence the material performance [14]. Properties such as compressive or flexural strength, hardness and Young's modulus improve as the filler content increases and polymerization shrinkage decreases. Reinforcement of dental fillers with mesoporous fibers [15], glass fibers [16], networked fibers [17], microparticles [18] and whiskers [19] have been demonstrated to result in dramatic improvements on the physical and mechanical properties. As a result, investigations on the potential of alternative reinforcing agents are ongoing.

Interestingly, short fibers of alumina, silk, ceria, etc. could be explored as reinforcement owing to their improved mechanical properties, resemblance in colour, semi-translucency in blend and are already used in the biomaterials field for various applications. Studies also revealed that the impregnation of extremely strong ceramic fibers/whiskers could lead to a two fold increase in RBC strength and toughness, as well as provide promising results in composite polish ability, water absorption and strength durability [20,21]. The advantage of silk fiber in dental resin composites are high strength, weight reduction, environmentally friendliness, skin-irritation free and good at interfacial bonding with resin matrix. Most importantly, it is cost effective, easily processable and biodegradable. Also ceria, an important rare-earth material can be applied as reinforcement in the form of nanofibers because of their high specific surface area-to volume ratio.

Herein for the first time, we have used alpha alumina microfibers, silk microfibers and ceria nanofibers as reinforcement in composite resins for dental filler. Therefore, the aim of this study is to investigate whether the addition of Alpha Alumina Microfibers (AMFs), Silk Microfibers (SMFs) and Ceria Nanofibers (CNFs) in formulation of flowable RBC would significantly enhance their physical/mechanical properties in the development of composite dental fillers.

2. Materials and methods

2.1. Alumina fiber by wet spinning

Alumina fibers were prepared as described in our previous work [22]. Briefly, homogenous slurry of aluminium hydroxide (Merck, Mumbai, India) containing 4 wt% chitosan (dissolved in 2 vol% acetic acid) in the ratio 1:10 was prepared by rotary ball-milling at 25 rpm for 24 h. The prepared slurry was made bubble free by addition of antifoaming agent (n-octanol) during agitation/milling and the slurry was flowable. For alumina fiber preparation, the slurry was filled into a 50 mL syringe and spun through a stainless

steel spinneret with average hole diameter of $\sim 100\ \mu\text{m}$. The syringe was pushed through a pneumatic piston under 0.3 MPa pressure and the slurry was extruded to a coagulation bath (5 wt% aqueous STPP; pH ~ 8.6) to form fibers. Alumina fibers were washed thoroughly with distilled water and dried in a controlled humidity cabinet at 50 °C. Finally, the fibers were fully dried under vacuum chamber following binder burn out and sintering in a chamber furnace (Bysakh, Kolkata, India) in presence of air. For binder burn out and sintering, the following temperature schedule was used. Initially, the heating rate of 1 °C/min was employed up to 550 °C with dwelling time of 1 h, 0.5 h at 300 °C and 450 °C, respectively, which was followed by the heating rate of 6 °C/min and 3 °C/min up to 1000 °C and 1550 °C, respectively, with dwelling time of 2 h at final temperatures.

2.2. Processing of silk fiber

Silk cocoons were processed into short fibers as described elsewhere [23]. Briefly, cocoons of *Bombyx mori* silkworm were chopped into small pieces and degummed in boiling 0.02 M sodium carbonate solution for 30 min. They were washed thoroughly in deionized water and air dried. The air dried degummed silk fibers (0.35 g) were hydrolysed for 30 s by addition of 17.5 M sodium hydroxide solution with constant stirring. To stop hydrolysis, excess water was added to the reaction mixture and centrifuged at 5000 rpm for 5 min. Supernatant was discarded and the fibers were suspended in 50 mL of water, stirred, and centrifuged. This step was repeated for 5 times to remove excess NaOH and pH was adjusted to 7.0 using hydrochloric acid. The neutralized fiber solution was again centrifuged at 5000 rpm for 5 min and resuspended in water (repeated five times). Finally, the fibers were suspended in PBS and lyophilized to generate a silk-fiber powder.

2.3. Ceria nanofiber by electrospinning

The solution of cerium nitrate (1.0 g $\text{Ce}(\text{NO}_3)_3 \cdot 6\text{H}_2\text{O}$ and 4.0 ml of H_2O) was added slowly into 30 ml of aqueous polyvinyl alcohol solution of 7 wt%, and the reaction proceeded in a water bath at 50 °C for 5 h. Thus, a viscous gel of PVA/cerium nitrate was obtained. The viscous gel of PVA/cerium nitrate was contained in a plastic syringe with a blunt needle connected to a high-voltage generator. A grounded iron drum collector, covered with an aluminium foil, served as counter electrode. A voltage of 21 kV was applied to the gel and a dense web of fibers was collected on the aluminium foil. The fibers thus formed were calcined at a rising rate of 240 °C/h and remained for 3 h at 800 °C.

2.4. X-ray Diffraction Analysis

For phase analysis of the alumina, ceria, silk fibers, X-ray diffraction experiments were carried out using Mo-filtered Cu K α radiation at a scanning rate of 3°/min between 20° and 80° by X'Pert Pro PANalytical (Model PW3040/60, Almelo, the Netherlands).

2.5. Measurement of degree-of-conversion

Degree of photopolymerization is directly related to extent of conversion, which is important for improving mechanical properties. However, the degree of polymerization suffers from fillers loading due to lesser penetration of photons. Thus, extent of fiber loading in the composite was determined by the degree of photopolymerization conversion of specimens containing alumina/silk/ceria fibers in the present study. The test specimens were placed between two thin glass plates, pressed to form a very thin film and the absorbance peaks of the un-cured samples were obtained. The specimens with different wt% of fibers were then light-cured

for 2 min using the light source and the peaks were collected for the cured specimens. Degree of conversion (DC%) was determined from the ratio of absorbance intensities of aliphatic C–C (peak at 1638 cm^{-1}) against internal reference of the aromatic C–C (peak at 1608 cm^{-1}) before and after curing of the specimen. The degree of conversion was then calculated as follows:

$$\text{DC}\% = \frac{1 - (1638\text{ cm}^{-1}/1608\text{ cm}^{-1}) \text{ peak area after curing}}{(1638\text{ cm}^{-1}/1608\text{ cm}^{-1}) \text{ peak area before curing}} \times 100$$

For each group of fiber resin composites, the measurement was repeated five times.

2.6. Viscosity study of fiber resin mixture

Viscosity analysis of the dental resin with different ratios of alumina/silk/ceria fibers [(10% Alumina Microfibers (AMFs), 5% Silk Microfibers (SMFs), and 3.33% Ceria Nanofibers (CNFs)] were carried out to understand the flow behaviour of the dental resin mixtures. Viscosities of different slurries were measured at shear rates ranging between 0.5 and 100 s^{-1} at $25\text{ }^{\circ}\text{C}$ using Bohlin CVO Rheometer (Malvern Instrument, UK) with a parallel plate geometry (20 mm diameter spindle) maintaining a gap of $500\text{ }\mu\text{m}$.

2.7. Preparation of fiber reinforced dental composites

The base resin consisted of 49.5% Bis-GMA (Sigma–Aldrich), 49.5% TEGDMA (Sigma–Aldrich) making a 50/50 mass ratio of Bis-GMA/TEGDMA, 0.2% CQ (Sigma–Aldrich) and 0.8% 4EDMAB (Sigma–Aldrich). Prior to fabrication of composites, the base resin pastes were exposed to a reduced pressure of ~ 0.5 atmosphere for ~ 1 min to reduce the amount of air bubbles that had been entrapped during mixing. The base resin was mixed with different mass fractions of uniformly crushed 10% AMFs, 5% SMFs, 3.33% CNFs. The dental resin fiber mixture was then transferred to ultraviolet crosslinker to be photocured for 2 min. The preparations of dental composites were conducted in dark room to avoid premature curing.

2.8. Measurement of the depth of cure

The depth of cure of resin composite was determined as described elsewhere [24]. The composite resins containing alumina/silk/ceria fibers were casted into a metallic mould with a cylindrical cavity of 10 mm height and 4 mm diameter while the top of the mould were covered with transparent polymer sheet. The specimens were then photocured for 2 min through UV exposure from the top. Immediately after irradiation, uncured materials were scraped away with a plastic spatula. Subsequently, the height of the cured resin was measured in three different places using a digital micrometre. The measured values were divided by 2 and the average of three measurements was then reported as the depth of cure.

2.9. Artificial saliva preparation and mass change behaviour of the fibers resin composites in artificial saliva

Artificial saliva was prepared according to Macknight-Hane and Whitford formula and pH of the saliva was adjusted to 6.75 with KOH [25]. The composition of saliva is shown in Table 1.

Mass change behaviour of the resin composites made from 10% AMFs, 5% SMFs and 3.33% CNFs was evaluated in artificial saliva, at pH 6.75 at $37\text{ }^{\circ}\text{C}$. After drying in air at $37\text{ }^{\circ}\text{C}$ for 1 week, the initial mass of each group, m_0 , was determined using an analytical balance (Mettler-Toledo International Inc., Columbus, OH, United

Table 1
Composition of the prepared artificial saliva.

S. No.	Composition	Grams per liter
1	Methyl-p-hydroxybenzoate	2.00
2	Sodium carboxymethyl cellulose	10.00
3	KCL	0.625
4	MgCl ₂ ·6H ₂ O	0.059
5	CaCl ₂ ·2H ₂ O	0.166
6	K ₂ HPO ₄	0.804
7	KH ₂ PO ₄	0.326

States of America), with a precision of ± 0.01 mg. They were then separately placed in the prepared artificial saliva, and their mass change was monitored and recorded at regular intervals. After removing and blotting dry with filter paper to remove surface adherent liquid, the samples wet mass (m_t) was determined, and they were placed immediately to the solution. After the end of the test time (30 days), the mass change was calculated from the formula below

$$\text{Change in mass (\%)} = \frac{m_t - m_0}{m_0} \times 100$$

2.10. Three-point flexural test and compressive strength measurement

To prepare the specimens for three-point flexural and crushing tests, the base resin along with different ratios of uniformly crushed fibers [10% AMFs, 5% SMFs and 3.33% CNFs] were photocured in Teflon moulds to get the required dimension for mechanical testing. Prior to mechanical testing, the photocured specimens were stored in a humidifier at $37\text{ }^{\circ}\text{C}$ for 24 h. Ten specimens were prepared for each measurement, and the specimens were carefully hand-polished with silicon carbide paper. A standard three-point flexural test (ASTM D 790) was used to fracture the specimens (span: 35 mm; width: 5 mm; depth: 3.5 mm) at a crosshead speed of 0.5 mm/min using a computer controlled universal testing machine (Hounsfield, UK).

For compressive strength measurement, cylindrical samples (diameter: 12.5 mm) of cross-sectional area 122.7 mm^2 were evaluated for crushing strength by universal testing machine (25 K machine, Hounsfield, UK) at crosshead speed of 0.5 mm/min using 25,000 N load cell. Flexural strength (FS), elastic modulus (ES), work-of-fracture (WOF) and compressive strength (CS) of the base dental resins without fibers (control) and the corresponding composites (containing 10% AMFs, 5% SMFs and 3.33% CNFs) were tested.

2.11. Microstructure analysis

Scanning electron microscopy (SEM; EVO ZEISS, Carl Zeiss SMT AG, Oberkochen, Germany) of the fabricated alumina/silk/ceria fibers and fracture surface of resin composites were carried out to examine their microstructures. Briefly, fully dried samples were placed on a sample holder using carbon coated double-sided tapes. The samples were further gold coated using plasma coater for 30 s under high vacuum to avoid charging effect.

2.12. Adhesive strength measurement

The dental resins composites containing (wt%) 10% AMFs, 5% SMFs and 3.33% CNFs were tested for their adhesive strength. Briefly, dental crowns were collected from cadaver and a 0.5 mm diameter hole was made by CNC machine using a diamond embedded tool fabricated from our previous work [26]. Then the cylindrical

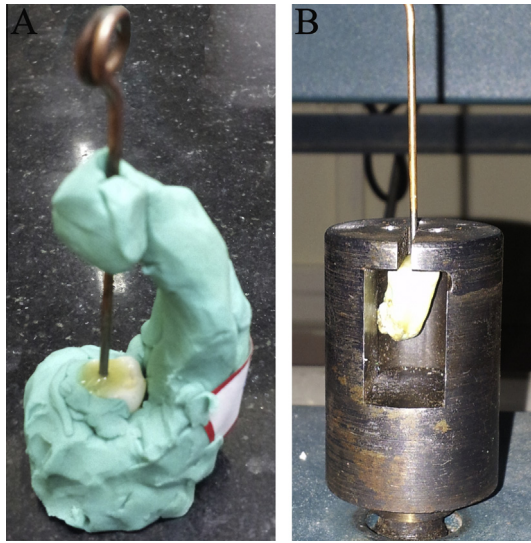


Fig. 1. Images of (A) sample preparation setup and (B) modified sample holder used for adhesive strength measurement.

insert as shown in Fig. 1A is attached to it by applying the composite resins mixtures and photocured for 2 min. The photocured samples were incubated at 37 °C in a water bath for 30 days. Modified sample holder (Fig. 1B) was used and the samples before and after incubation in artificial saliva were tested using universal testing machine (25 K machine, Hounsfield, UK) in tensile mode. Adhesive strength is calculated using the formula below-

$$\text{Adhesive strength} = \frac{\text{Load at failure}}{\text{Area of the insert embedded inside the dental crown}}$$

2.13. Data analysis

The data were analysed using GraphPad Prism software (version 5.02, La Jolla, CA, USA) by one-way ANOVA, Dunnett’s multiple comparison Test. The level of significance was determined as $P < 0.05$ significance.

3. Results

3.1. Morphology of the alumina, silk and ceria fibers

The SEM micrographs of the fabricated AMFs, SMFs and CNFs samples are shown in Fig. 2. The fibers were well separated as shown in micrograph. The average diameter of the fabricated alumina fibers after sintering varied between 70 and 120 μm and the fibers exhibited intercalated hexagonal platelet morphology. In case of silk and ceria fibers, the average diameter was found to be ~10 μm and ~200 nm, respectively. All the samples were sieved for their uniformity in size and within 50 mesh (297 μm)–60 mesh (250 μm) cut-off fibers were used for further studies.

3.2. X-ray Diffraction Analysis

XRD patterns of the fabricated alumina, silk and ceria fibers are shown in Fig. 3. The alumina fibers displayed XRD peaks at 2θ values of 25°, 35°, 38°, 43°, 46°, 52°, 57°, 59°, 61°, 66°, 68°, 70°, 74°, and 77° (JCPDS No. 78-2427) which correspond to alpha alumina phase and several small intensity peaks appeared for an unknown phase. The silk fibers exhibited a major X-ray diffraction peak at 20.5°, which is characteristic of silk with highly ordered β-sheet structure. Ceria fibers revealed strong diffraction peaks corresponding to CeO₂ at 2θ values of 28.68, 33.18, 47.58, 56.58, 59.28, and 69.48 respectively (JCPDS No. 34-0394) indicating presence of cubic fluorite structure.

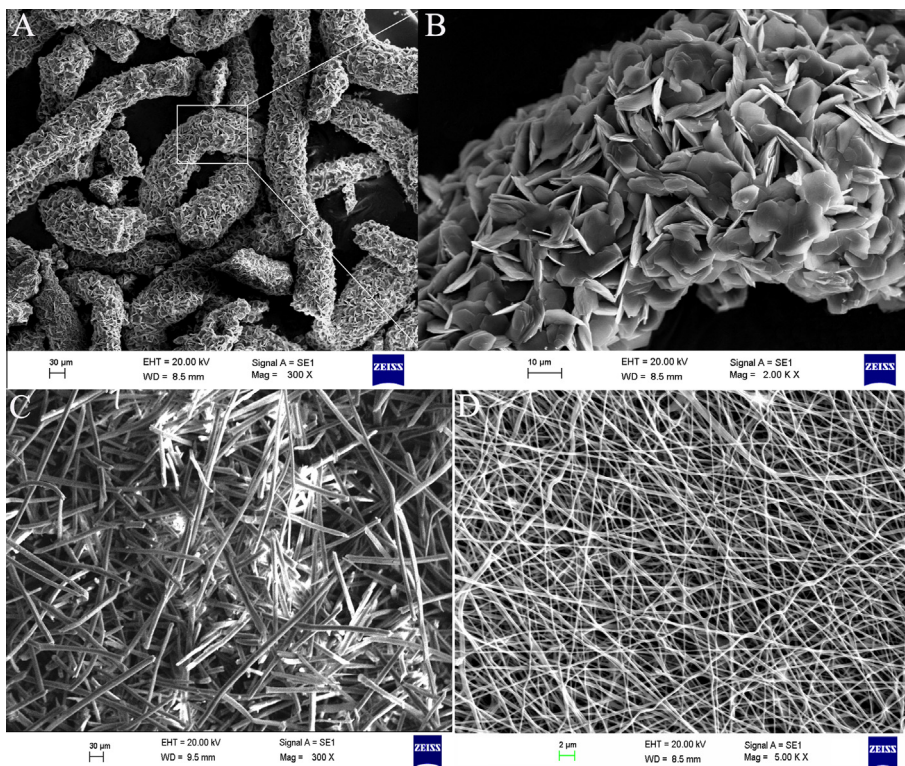


Fig. 2. SEM micrographs of fabricated fibers (A) and (B) representative of alumina microfibers at different magnifications; (C) silk micro fibers and (D) ceria nanofibers.

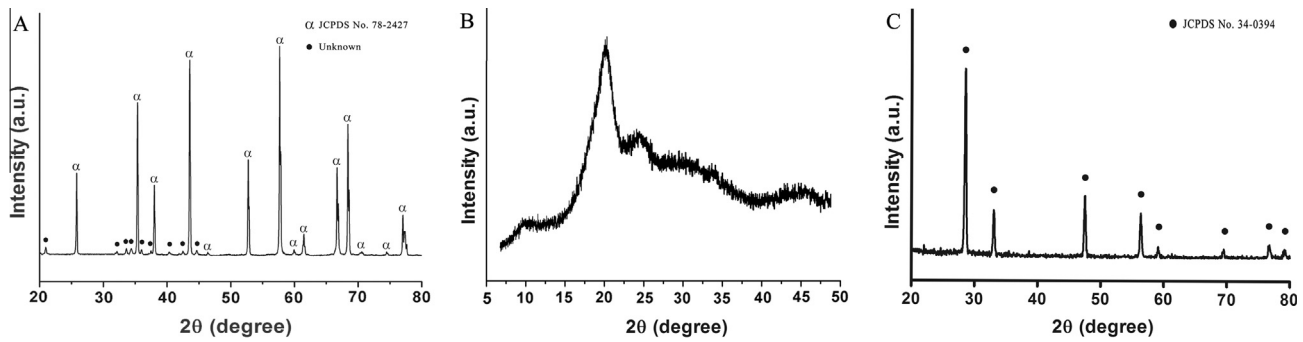


Fig. 3. XRD patterns of sieved short fibers (A) alumina fiber (B) silk fiber and (C) ceria fiber used for preparation of composites.

3.3. Measurement of degree-of-conversion

After preliminary work [data not shown], the maximum wt% of the fiber that can be added for the fabrication of fiber-resin composites without affecting the degree of conversion was determined as 10% AMFs, 5% SMFs and 3.33% CNFs. As described in the experimental section, the degree of conversion was quantified using FTIR spectroscopy data as displayed in Fig. 4 (as the mean values of DC% in four groups). Dunnett's multiple comparison test revealed that there was no significant difference ($p > 0.05$) between the DC% of the groups containing 10% AMFs, 5% SMFs and 3.33% CNFs compared to control. Here, it is important to mention that the diameter of the fibers played a major role in determining their loading percentage during preparation of composites. The CNF fibers exhibited high volume due to their nanometer range diameter, which eventually restricted their loading during mixing associated with rapid rise in viscosity. Further, the degree of conversion was also affected for this composite and 3.33% CNFs loading was optimized for similar conversion with control. The maximum fiber loading [10% AMFs, 5% SMFs and 3.33% CNFs] was used in further experiments as determined from degree of conversion analyses.

3.4. Viscosity study of fiber resin mixture

The viscosities of the fiber resin mixture at different shear rate are shown in Fig. 5. The photo curable composite resin mixtures made using 10% AMFs, 5% SMFs, and 3.33% CNFs demonstrated shear thinning behaviour against different shear rates. The viscosity of base resin at shear rate 10 (1/s) was found to be 2.48 Pa s and for resin mixture with 10% AMFs, 5% SMFs and 3.33% CNFs were 6.24, 7.93 and 4.55 Pa s, respectively.

3.5. Measurement of the depth of cure

The mean depths of cure values are shown in Fig. 6. There was a significant difference ($p < 0.05$) in depth of cure values of all groups. It is noted that addition of small amount of fibers affected the curing depth.

3.6. Mass change behaviour of the fibers resin composites in artificial saliva

All groups, including the base resin, demonstrated an initial rapid increase in mass, as shown in Fig. 7. The highest saliva uptake was appeared to be at ~ 10 days and after 10 days there was no further increase in mass which may be due to elution from the samples. Compared with the control, groups containing (wt%) 10% AMFs, 5% SMFs and 3.33% CNFs demonstrated less water-uptake in 30 days, and the rate of change in mass decreased with addition of short fibers. Group with 5% SMFs showed a higher water uptake than those filled with 10% AMFs and 3.33% CNFs, but no further

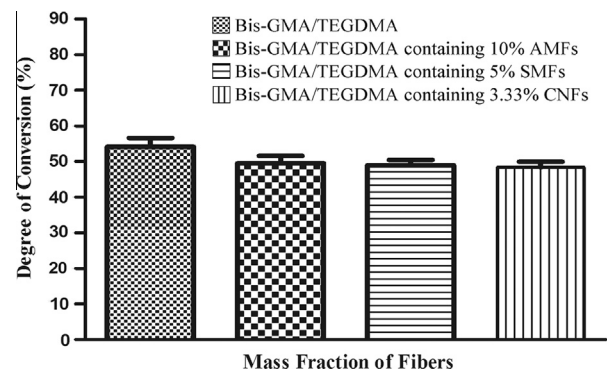


Fig. 4. Degree of conversions of resin composites containing (wt%) 10% AMFs, 5% SMFs and 3.33% CNFs. Y-error bars represent standard deviation.

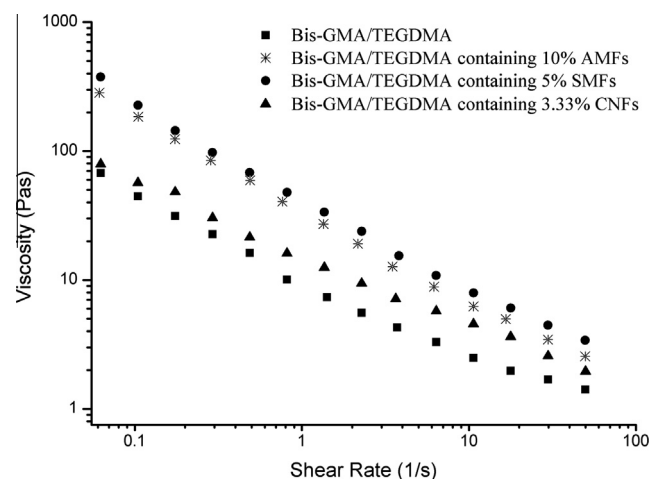


Fig. 5. Viscosity diagram of fiber-resin mixtures containing (wt%) 10% AMFs, 5% SMFs and 3.33% CNFs compared with base resin at different shear rates.

detail could be extracted by further analysis of these data. Long-term exposure is necessary for more critical evaluation.

3.7. Flexural strength and elastic modulus

As shown in Fig. 8A and B, there was a significant difference ($p < 0.05$) in flexural strength and elastic modulus of the groups containing (wt%) 10% AMFs, 5% SMFs and 3.33% CNFs, compared to the control. Incorporation of the short fibers into the resin composite resulted in an increase in the flexural strength and elastic modulus of the composites with a maximum corresponding to the group containing 5% SMFs followed by 10% AMFs and 3.33% CNFs.

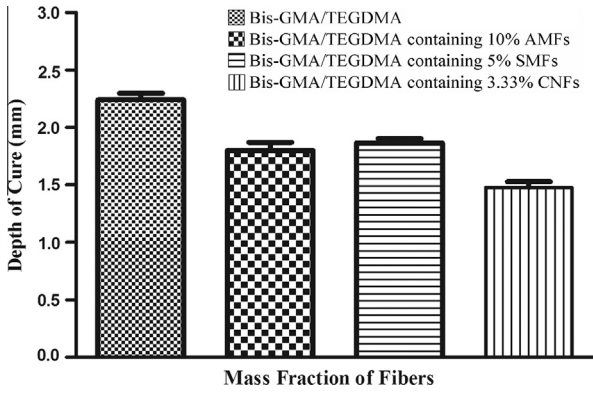


Fig. 6. Depth of cure (mm) of resin composites containing (wt%) 10% AMFs, 5% SMFs and 3.33% CNFs compared with base resin. Y-error bars represent standard deviation.

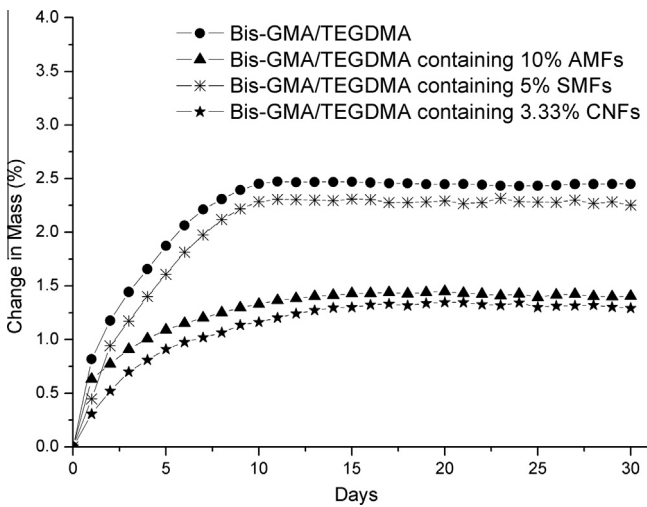


Fig. 7. Variation in% mass change of the composites containing (wt%) 10% AMFs, 5% SMFs, 3.33% CNFs with immersion time in artificial saliva at 37 °C compared with base resin.

SEM images of fracture surfaces (Fig. 9) shows that composites containing 10% AMFs, 5% SMFs and 3.33% CNFs had different failure modes from that of the base resin. Plastic deformation (PD), Cone cracking (CC), radial cracking (RC) appeared in all specimens. Fiber pullout (FP) was also seen in composites containing fibers.

3.8. Compressive strength and work-of-fracture

The Compressive strength and work-of-fracture of the resin composites containing (wt%) 10% AMFs, 5% SMFs, 3.33% CNFs were

measured and the results are shown in Fig. 10A and B. As expected, there was an increase in the compressive strength and work-of-fracture of the resin composite groups containing AMFs, SMFs and CNFs. Statistical comparison also revealed significant difference between the composites of different groups ($p < 0.05$).

3.9. Adhesive strength measurement

Adhesive strengths of composites containing (wt%) 10% AMFs, 5% SMFs, 3.33% CNFs and base resin after 30 days of incubation in artificial saliva are shown in Fig. 10C. With composites containing 10% AMFs & 5% SMFs, there was a significant improvement in adhesive strength ($p < 0.05$) with addition of short fibers into base resin. In contrast, the composite containing 3.33% CNFs had no significant increments in the adhesive strength ($p > 0.05$) as compared with base resin. Adhesive strength data of composites before incubation in artificial saliva (data not shown) did not reveal any significant difference ($p > 0.05$) when compared to the data after 30 days of incubation in artificial saliva.

4. Discussion

The motivation of the current study was to incorporate short fibers like AMFs, SMFs and CNFs into the flowable dental resin to significantly increase the mechanical properties of the resulting composites to facilitate effective reinforcement of dental filler. Good dispersion of the fibers in the polymer matrix is considered to be an important criteria for obtaining improved mechanical performance. Also at high fiber loading, it is proved that lack of fiber dispersion can result in agglomeration of fibers which has direct effect to reduce the reinforcing potential of the composites [27,28]. Three different materials with varying diameters (e.g., AMFs with ~120 μm, SMFs with ~10 μm and CNFs with ~200 nm) were evaluated for their reinforcement efficacy as dental filler. Among them, the natural biopolymer based silk fiber, used widely in biomedical applications, is compared with synthetic ceramic based alumina and ceria fibers. The silk fibers had smooth surface appearance due to the native biospinning procedure compared to sintered alumina and ceria fibers. The surface roughness of the sintered alumina fibers was associated with hexagonal platelet like grain boundary formation. In case of CNFs, the defects were relatively smaller due to finer diameter and smaller grain size. Using these fibers as reinforcement, physico-mechanical performances of the composite dental fillers were optimized by varying percent fiber loading, degree of conversion, depth of cure and their reinforcement efficacy was compared with base resin. It is to be noted that there were no significant reduction in the degree of conversion during photopolymerization up to addition of (wt%) 10% AMFs, 5% SMFs and 3.33% CNFs to the base resin and all the

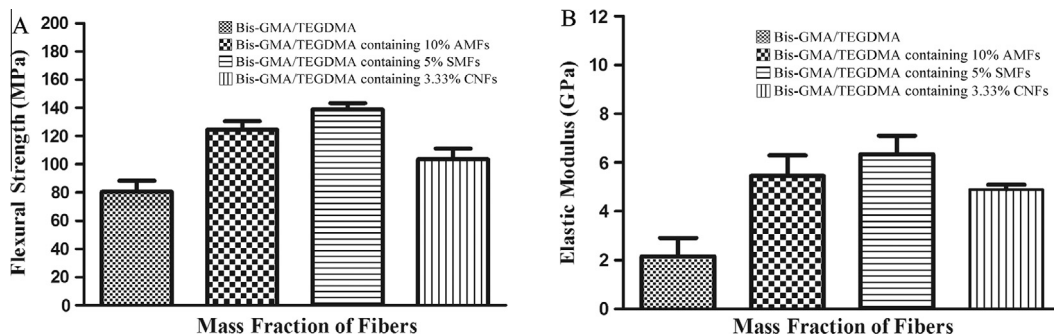


Fig. 8. (A) Flexural strength (MPa) and (B) elastic modulus (GPa) of composites containing (wt%) 10% AMFs, 5% SMFs, 3.33% CNFs compared with the base resin. Y-error bars represent standard deviation.

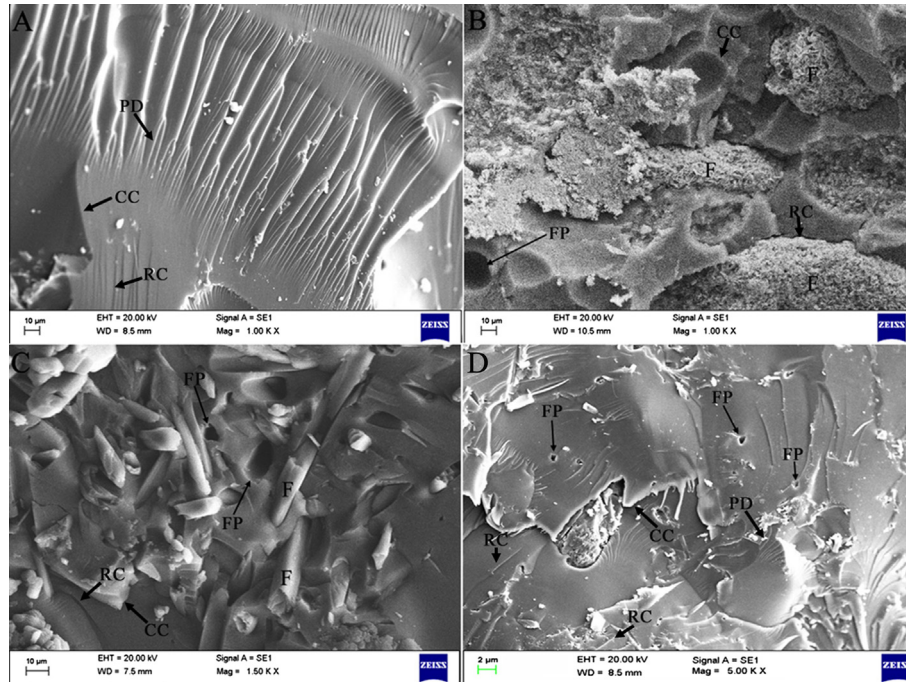


Fig. 9. Microscopic fracture patterns of (A) base resin, (B) composites containing (wt%) 10% AMFs, (C) composites containing 5% SMFs and (D) composites containing 3.33% CNFs (CC: cone cracking, PD: plastic deformation, RC: radial cracking, FP: fiber pullout, F: fiber).

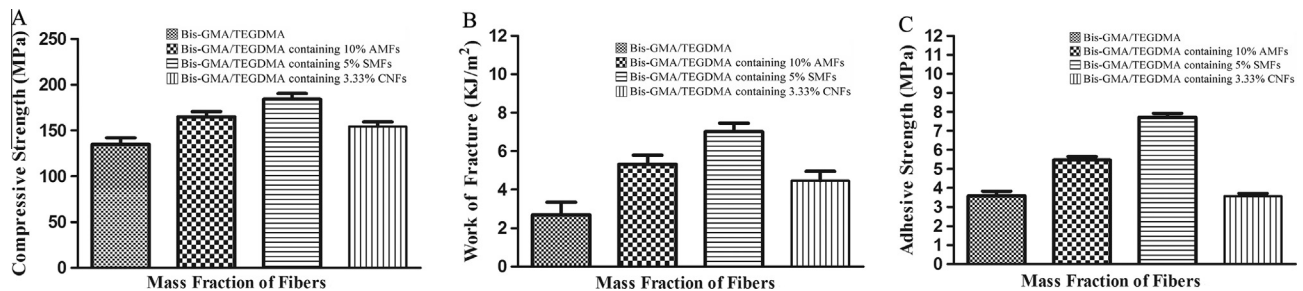


Fig. 10. (A) Compressive strength (MPa), (B) work-of-fracture (kJ/m²) and adhesive strength (MPa) of the base resin and composites containing (wt%) 10% AMFs, 5% SMFs, 3.33% CNFs. Y-error bars represent standard deviation.

further studies were extended using the said compositions for respective fibers (Fig. 4) for their comparisons.

Resin mixtures made from 10% AMFs, 5% SMFs, and 3.33% CNFs prior to curing were flowable and demonstrated non Newtonian and shear thinning behaviour (Fig. 5) which eventually offered easy filling to the cavities and gaps in complex clinical situations. Depth of cure obtained after curing the resin is considered to be a critical parameter for dental filler application in clinical practice, since in complicated cases curing source may not reach to the location to be restored. The result of the current study revealed that incorporation of (wt%) 10% AMFs, 5% SMFs, 3.33% CNFs into the resin mixtures decreased the depth of cure compared to the base resin (Fig. 6). In this context, Le Bell et al. have demonstrated that glass fiber-reinforced composite has higher light penetration with better curing compared to conventional composite resin [29]. However, the fibers used in the current study have higher light scattering phenomena, which resulted in lower depth of cure. Thus, further optimization in fraction of fiber loading is necessary for improving depth of cure. Also, fiber loading wt% was varied for obtaining similar degree of conversion owing to difference in diameter and volume fraction of fibers.

The behaviour of dental composites in wet environment is of great significance as the composites always perform in the presence

of saliva. It has been previously demonstrated that water sorption can affect the mechanical properties and stability of the composites [30]. Consequently, this property leads to the decrease in the filler matrix interface, thus affecting the life span of resin composites. Diffusion of saliva in the matrix also depends on degree of polymerization and filler volume fraction. In the present study, samples containing 5% SMFs showed a higher saliva uptake than those filled with 10% AMFs and 3.33% CNFs (Fig. 7). This may be due to swelling of silk fibroin associated with hydrophilic moieties [31]. In case of composites containing 10% AMFs and 3.33% CNFs, the saliva uptake is less due to absence of swelling of ceramic reinforcements.

The reinforcing effect of the fiber fillers is mainly due to the transfer of stress from resin matrix to fibers and also because of the individual fiber acts as bridge in the crack path. In this context, Garoushi et al. demonstrated the reinforcement mechanism of short fibers during their application as dental filler [32]. SEM microscopy of the fracture surface (Fig. 9) revealed that the composites cracked surfaces were very rough, while in contrast, the fracture surface of the control sample was very smooth with much larger plastic deformation suggesting the role of effective crack deflection by fibers in case of composites. Also in the event of crack propagating away from the fibers, numerous fracture lines and steps were generated

on the fracture surface, signifying energy consumption during the failure. In addition to the energy absorption mechanisms of the resin itself, increased work of fracture was required due to the expected reinforcing and toughening mechanisms, i.e. crack deflection, crack bridging or pinning, and fiber pullout.

In base resin (Fig. 9A), CC and PD were dominant with only rare bottom initiated RC. In case of composites containing 10% AMFs (Fig. 9B) very few FPs were seen with majority of fibers embedded firmly in the matrix preventing crack propagation through them. In 5% SMFs (Fig. 9C), CC and RC prevailed and the fibers were randomly distributed in the composites, with no appreciable debonding, resin-filler gaps, or voids on the fracture surface. Also FP was evidently more which has direct effect on the improved mechanical properties. In 3.33% CNFs (Fig. 9D) CC, RC, FP and PD could be detected with uneven dispersion and orientation of the fibers. This condition may be attributed to the high surface area-to volume ratio of CNFs and also due to the processing conditions. Other possible reason for uneven distribution of CNFs in the resin matrix may be due to improper mixing of CNFs to the base resin prior to photo curing because of the limitations of hand-mixing.

Flexural strength (FS), elastic modulus (EM), compressive strength (CS), work-of-fracture (WOF) and adhesive strength (AS) of the composites were all substantially increased by impregnation of 10% AMFs, 5% SMFs and 3.33% CNFs in the base dental resin (Figs. 8 and 10). For 10% AMFs reinforced composite FS, EM, CS, WOF and AS values (mean \pm standard deviation, $n = 10$) were 125 ± 14.9 MPa, 5.5 ± 1.9 GPa, 165.2 ± 12 MPa, 5.3 ± 1 kJ/m² and 5.47 ± 0.3 MPa, respectively. In case of 5% SMFs reinforced composite, the FS, EM, CS, WOF and AS values were 138 ± 11 MPa, 6.34 ± 1.7 GPa, 184.2 ± 14 MPa, 7.0 ± 0.9 kJ/m² and 7.7 ± 0.38 MPa, respectively and 3.33% CNFs reinforced composite the values were 103 ± 18.52 MPa, 4.89 ± 0.43 GPa, 154.5 ± 11.25 MPa, 4.46 ± 1.10 kJ/m² and 3.58 ± 0.26 MPa, respectively. In control samples, FS, EM, CS, WOF and AS values were 80.5 ± 7.84 MPa, 2.152 ± 0.75 GPa, 154.5 ± 11.25 MPa, 4.46 ± 1.10 kJ/m² and 2.68 ± 0.66 MPa, respectively. Possible reasons for the improvement of the mechanical properties of the fiber reinforced composite are (1) strong bonding between fibers and resin; (2) the fiber moduli was higher than the resin matrix; and (3) also some weakly bonded fibers to the resin matrix were pulled out under load. Moreover being a natural fiber of protein origin, the silk may have promoted better interaction with the resin matrix causing superior mechanical properties and improved performance while compared with the composite made of fragile ceramic fibers as reinforcement.

5. Conclusion

In this study, addition of different short fibers such as AMFs, SMFs and CNFs into Bis-GMA/TEGDMA resins with optimized fiber-resin composition had significant flow ability and are photocurable. The degree of conversion and depth of cure were reduced with addition of short fibers into base resin during formulation of composites. Also, impregnations of 10% AMFs, 5% SMFs, 3.33% CNFs into the base resins provided similar degree of conversion but depth of cure was affected. The resultant composites had significant improvement in mechanical properties in comparison to base resin for both alumina and silk as additives. The adhesive strength of composites reinforced with 3.33% CNFs did not improve significantly due to aggregation of nanofibers during mixing with the resin matrix. AMFs, SMFs and CNFs reinforced composite resins revealed significant improvements in physical and mechanical properties indicating their plausible application as additives in composite dental filler.

Acknowledgments

Fellowship from Council of Scientific and Industrial Research (CSIR), Govt. of India, New Delhi is acknowledged for Arun Prabhu Rameshbabu and Paulomi Ghosh. Fellowship from Department of Science and Technology (DST) is acknowledged for Kamakshi Bankoti. Financial aid from DST, Defence Research & Development Organisation (DRDO), and CSIR, Govt. of India, New Delhi is acknowledged.

References

- Lin D, Li Q, Li W, Zhou S, Swain MV. Design optimization of functionally graded dental implant for bone remodeling. *Composites Part B* 2009;40:668–75.
- Bharti R, Wadhvani KK, Tikku AP, Chandra A. Dental amalgam: an update. *J Conserv Dent* 2010;13(4):204–8.
- Rathore M, Singh A, Pant VA. The dental amalgam toxicity fear: a myth or actuality. *Toxicol Int* 2012;19(2):81–8.
- Muhamedagic B, Muhamedagic L, Masic I. Dental office waste – public health and ecological risk. *Mater Sociomed* 2009;21(1):35–8.
- Okabe T, Elvebak B, Carrasco L, Ferracane JL, Keanini RG, Nakajima H. Mercury release from dental amalgams into continuously replenished liquids. *Dent Mater* 2003;19(1):38–45.
- Xia Y, Zhang F, Xie H, Gu N. Nanoparticle-reinforced resin-based dental composites. *J Dent* 2008;36(6):450–5.
- Malhotra N, Mala K, Acharya S. Resin-based composite as a direct esthetic restorative material. *Compend Cont Educ Dent* 2011;32(5):14–23.
- Bindu MG, Satapathy BK, Jaggi HS, Ray AR. Size-scale effects of silica on bis-GMA/TEGDMA based nanohybrid dental restorative composites. *Composites Part B* 2013;53:92–102.
- Cramer NB, Stansbury JW, Bowman CN. Recent advances and developments in composite dental restorative materials. *J Dent Res* 2011;90(4):402–16.
- Navimipour EJ, Chaharom MEE, Oskoe PA, Mohammadi N, Bahari M, Firouzmandi M. Fracture resistance of endodontically-treated maxillary premolars restored with composite resin along with glass fiber insertion in different positions. *J Dent Res Dent Clin Dent Prospects* 2012;6(4):125–30.
- Zhang H, Darvell BW. Failure and behavior in water of hydroxyapatite whisker-reinforced bis-GMA-based resin composites. *J Mech Behav Biomed Mater* 2012;10:39–47.
- Garoushi S, Säilynoja E, Vallittu PK, Lassila L. Physical properties and depth of cure of a new short fiber reinforced composite. *Dent Mater* 2013;29(8):835–41.
- Leprince JG, Palin WM, Hadis MA, Devaux J, Leloup G. Progress in dimethacrylate-based dental composite technology and curing efficiency. *Dent Mater* 2013;29(2):139–56.
- Satterthwaite JD, Maisuria A, Vogel K, Watts DC. Effect of resin-composite filler particle size and shape on shrinkage-stress. *Dent Mater* 2012;28(6):609–14.
- Samuel SP, Li S, Mukherjee I, Guo Y, Patel AC, Baran G, et al. Mechanical properties of experimental dental composites containing a combination of mesoporous and nonporous spherical silica as fillers. *Dent Mater* 2009;25(3):296–301.
- Abdulmajeed AA, Närhi TO, Vallittu PK, Lassila LV. The effect of high fiber fraction on some mechanical properties of unidirectional glass fiber-reinforced composite. *Dent Mater* 2011;27(4):313–21.
- Garoushi S, Vallittu PK, Watts DC, Lassila LV. Polymerization shrinkage of experimental short glass fiber-reinforced composite with semi-inter penetrating polymer network matrix. *Dent Mater* 2008;24(2):211–5.
- Profeta AC, Mannocci F, Foxton R, Watson TF, Feitosa VP, De Carlo B, et al. Experimental etch-and-rinse adhesives doped with bioactive calcium silicate-based micro-fillers to generate therapeutic resin-dentin interfaces. *Dent Mater* 2013;29(7):729–41.
- Xu HH, Eichmiller FC, Antonucci JM, Schumacher GE, Ives LK. Dental resin composites containing ceramic whiskers and pre-cured glass ionomer particles. *Dent Mater* 2000;16(5):356–63.
- Xu HH, Schumacher GE, Eichmiller FC, Antonucci JM. Strengthening composite resin restorations with ceramic whisker reinforcement. *Pract Periodont Aesthet Dent* 2000;12(1):111–6.
- Xu HH, Quinn JB, Smith DT, Giuseppetti AA, Eichmiller FC. Effects of different whiskers on the reinforcement of dental resin composites. *Dent Mater* 2003;19(5):359–67.
- Mohanty S, Rameshbabu AP, Dhara S. α -Alumina fiber with platelet morphology through wet spinning. *J Am Ceram Soc* 2012;95(4):1234–40.
- Mandal BB, Grinberg A, Gil ES, Panilaitis B, Kaplan DL. High-strength silk protein scaffolds for bone repair. *PNAS* 2012;109(20):7699–704.
- Tavassoli Hojati S, Alaghemand H, Hamze F, Ahmadian Babaki F, Rajab-Nia R, Rezvani MB, et al. Antibacterial, physical and mechanical properties of flowable resin composites containing zinc oxide nanoparticles. *Dent Mater* 2013;29(5):495–505.
- McKnight-Hanes MC, Leverett DH, Adair SM, Shields CP. Fluoride content of infant formulas: soy-based formulas as a potential factor in dental fluorosis. *Pediatr Dent* 1988;10(3):189–94.

- [26] Mohanty S, Rameshbabu AP, Dhara S. Net shape forming of green alumina via CNC machining using diamond embedded tool. *Ceram Int* 2013;39:8985–93.
- [27] Borrego LP, Costa JDM, Ferreira JAM, Silva H. Fatigue behaviour of glass fibre reinforced epoxy composites enhanced with nanoparticles. *Composites Part B* 2014;62:65–72.
- [28] Gamze Karsli N, Yesil S, Aytac A. Effect of hybrid carbon nanotube/short glass fiber reinforcement on the properties of polypropylene composites. *Composites Part B* 2014;63:154–60.
- [29] Le Bell AM, Tanner J, Lassila LV, Kangsniemi I, Vallittu PK. Depth of light-initiated polymerization of glass fiber-reinforced composite in a simulated root canal. *Int J Prosthodont* 2003;16(4):403–8.
- [30] Dhakal HN, Zhang ZY, Richardson MOW. Effect of water absorption on the mechanical properties of hemp fibre reinforced unsaturated polyester composites. *Compos Sci Technol* 2007;67(8):1674–83.
- [31] Cao Z, Chen X, Yao J, Huang L, Shao Z. The preparation of regenerated silk fibroin microspheres. *Soft Matter* 2007;3:910–5.
- [32] Garoushi S, Vallittu PK, Lassila LV. Short glass fiber reinforced restorative composite resin with semi-inter penetrating polymer network matrix. *Dent Mater* 2007;23(11):1356–62.